

# Flexible Conformal Highest Predictive Conditional Density Sets

Max Sampson

Department of Statistics and Actuarial Science, University of Iowa  
and

Kung-Sik Chan

Department of Statistics and Actuarial Science, University of Iowa

July 1, 2024

## Abstract

We introduce our method, conformal highest conditional density sets (CHCDS), that forms conformal prediction sets using existing estimated conditional highest density predictive regions. We prove the validity of the method and that conformal adjustment is negligible under some regularity conditions. In particular, if we correctly specify the underlying conditional density estimator, the conformal adjustment will be negligible. When the underlying model is incorrect, the conformal adjustment provides guaranteed nominal unconditional coverage. We compare the proposed method via simulation and a real data analysis to other existing methods. Our numerical results show that the flexibility of being able to use any existing conditional density estimation method is a large advantage for CHCDS compared to existing methods.

*Keywords:* Additive conformal adjustment; Highest density prediction; Kernel density estimation; Multi-modal predictive distribution.

# 1 Background

The problem of estimating upper-level or highest density sets has been widely studied [Polonik, 1995, Cuevas and Fraiman, 1997, Rigollet and Vert, 2009, Chen et al., 2017, Samworth and Wand, 2010, Lei and Wasserman, 2014]. It involves estimating  $\{x : f(x) > \lambda^{(\alpha)}\}$  for some  $\lambda^{(\alpha)} > 0$  and density  $f$  based only on samples drawn from  $f$ , where  $\lambda^{(\alpha)}$  is chosen such that  $\int_{\{x: f(x) \leq \lambda^{(\alpha)}\}} f(y) dy = \alpha$ . The unconditional density can also be replaced by a conditional density to find conditional density-level sets. Nearly all existing conformal methods that attempt to find highest density sets partition the data [Lei and Wasserman, 2014, Izbicki et al., 2022], so the observed coverage probability can vary a lot within each partition [Lei and Wasserman, 2014, Izbicki et al., 2022, Angelopoulos and Bates, 2021]. See [Vovk et al., 2005, Lei and Wasserman, 2012, Angelopoulos and Bates, 2021] for an introduction to conformal inference.

In Section 2 we propose a new method for estimating the highest predictive density set or region that only requires estimating the conditional density and the corresponding unconformalized highest density prediction sets. Our method provides an easy conformal adjustment to highest density sets that guarantees finite sample prediction set coverage without partitioning the data. Because our conformal score is so simple, it can be quickly combined with nearly any conditional density estimator to find conformal prediction regions; see Section S3 in the Supplementary Material for a review of conditional density estimation. In Section 3, we show that the proposed method attains the  $1 - \alpha$  unconditional coverage rate. Moreover, we show that the conformal adjustment is asymptotically negligible with large training and calibration data, if the conditional density estimation is consistent. Thus, the proposed method preserves  $1 - \alpha$  conditional coverage rate asymptotically, if the conditional density estimation is correctly specified, and guarantees  $1 - \alpha$  unconditional coverage, even if the conditional density estimation scheme is incorrectly specified. In Section 4, we also compare our method via simulation to HPD-split [Izbicki

et al., 2022], which, to our knowledge, is the only other conformal prediction method that attempts to use conformal prediction to calibrate a conditional density estimator without computing conformal prediction sets within partitions. We include a real data analysis in Section 5 and conclude in Section 6. All proofs are relegated to Section S5 in the online Supplementary Material.

## 2 Algorithm idea

We now describe our method, conformalized highest conditional density sets (CHCDS), which guarantees coverage for existing estimated conditional highest density predictive regions without creating partitions. As with other split conformal prediction methods, we begin by splitting our data into sets used for training and calibration. The training set is indexed by  $\mathcal{I}_{tr}$  and the calibration set by  $\mathcal{I}_{cal}$ . Given any conditional density estimating function,  $\mathcal{B}$ , we fit  $\hat{f}(\cdot | \mathbf{x})$  on the training data.

$$\hat{f} \leftarrow \mathcal{B}[\{(Y_i, \mathbf{X}_i) : i \in \mathcal{I}_{tr}\}]$$

Now, using the trained model, compute unadjusted  $1 - \alpha$  highest density prediction sets using  $\hat{f}(\cdot | \mathbf{X}_i)$  for each  $i \in \mathcal{I}_{cal}$ . Denote the density cutoff points as  $\hat{c}(\mathbf{X}_i)$ , whereas their true counterparts w.r.t.  $f(\cdot | \mathbf{X}_i)$  are denoted as  $c(\mathbf{X}_i)$ . Now, using these density cutoff points and the calibration set, compute the scores,

$$V_i = \hat{f}(Y_i | \mathbf{X}_i) - \hat{c}(\mathbf{X}_i), \forall i \in \mathcal{I}_{cal}. \tag{1}$$

Next, compute  $\hat{q} = \lfloor \alpha(n_{cal} + 1) \rfloor$ th smallest value of  $\{\mathbf{V}\}$ . For the new data point,  $\mathbf{X}_{n+1}$ , compute the unadjusted  $1 - \alpha$  highest density prediction set using  $\hat{f}(\cdot | \mathbf{X}_{n+1})$ . Denote the estimated cutoff point as  $\hat{c}(\mathbf{X}_{n+1})$ . The conformal prediction set then becomes

$$\mathbf{C}(\mathbf{X}_{n+1}) = \{y : \hat{f}(y | \mathbf{X}_{n+1}) > \hat{c}(\mathbf{X}_{n+1}) + \hat{q}\}.$$

For reference, the procedure is outlined in Algorithm 1. Intuitively, this method starts with an estimate of the highest density set. It then adjusts the cutoff point up or down based on the scores to achieve the desired coverage. This is similar in nature to conformalized quantile regression, but it adjusts vertically based on the density estimate instead of horizontally based on the true response [Romano et al., 2019]. A visual of how our score works as compared to that of HPD-Split can be seen in Section S1 in the Supplementary Material. The main advantages of CHCDS compared to other methods is that it does not partition the data and that it can easily be used with any existing conditional density estimator.

---

**Algorithm 1** CHCDS

---

**Input:** level  $\alpha$ , data  $\mathcal{Z} = (Y_i, \mathbf{X}_i)_{i \in \mathcal{I}}$ , test point  $(\mathbf{x})$ , and conditional density algorithm  $\mathcal{B}$

**Procedure:**

- 1: Split  $\mathcal{Z}$  into a training fold  $\mathcal{Z}_{tr} \triangleq (Y_i, \mathbf{X}_i)_{i \in \mathcal{I}_{tr}}$  and a calibration fold  $\mathcal{Z}_{cal} \triangleq (Y_i, \mathbf{X}_i)_{i \in \mathcal{I}_{cal}}$
- 2: Fit  $\hat{f} = \mathcal{B}(\{(\mathbf{X}_i, Y_i) : i \in \mathcal{I}_{tr}\})$
- 3: For each  $i \in \mathcal{I}_{cal}$ , use a root finding technique to estimate the shortest  $1 - \alpha$  upper-level density set using  $\hat{f}(Y|\mathbf{X}_i)$ . Denote the density cutoff points as  $\hat{c}(\mathbf{X}_i)$
- 4: For each  $i \in \mathcal{I}_{cal}$ , compute the scores  $V_i = \hat{f}(Y_i|\mathbf{X}_i) - \hat{c}(\mathbf{X}_i)$
- 5: Compute  $\hat{q} = \lfloor \alpha(n_{cal} + 1) \rfloor$ th smallest value of  $\{\mathbf{V}\}$
- 6: For the test point, use a root finding technique to estimate the shortest  $1 - \alpha$  set for  $\hat{f}(Y|\mathbf{x})$ . Denote the density cutoff point as  $\hat{c}(\mathbf{x})$

**Output:**  $\hat{C}(\mathbf{x}) = \{y : \hat{f}(y|\mathbf{x}) > \hat{c}(\mathbf{x}) + \hat{q}\}$

---

A problem can occur when the prediction level is high and the conditional density estimator overestimates the estimated density value cutoff for the unadjusted  $1 - \alpha$  prediction set. That is, the estimated prediction set under covers before the conformal adjustment. When this occurs, the final density cutoff for the new prediction point is a negative value, or

an infinite prediction set. The problem can be mitigated by using a multiplicative conformal adjustment in lieu of an additive conformal adjustment. However, the two approaches generally yield similar prediction sets, see Section S2 in the Supplementary Material for a detailed comparison.

### 3 Theoretical Properties

In this section, we study two theoretical properties of the proposed method. The following result establishes the coverage rate of the proposed method. All proofs are relegated to Section S5 in the Supplementary Material.

**Theorem 1.** *If  $(Y_i, \mathbf{X}_i), i = 1, \dots, n$  are exchangeable, then the prediction interval  $\hat{C}(\mathbf{X}_{n+1})$  constructed by CHCDS satisfies*

$$pr\{Y_{n+1} \in \hat{C}(\mathbf{X}_{n+1})\} \geq 1 - \alpha.$$

*If the  $V_i$ 's are almost surely distinct, then*

$$pr\{Y_{n+1} \in \hat{C}(\mathbf{X}_{n+1})\} \leq 1 - \alpha + (n_{cal} + 1)^{-1}.$$

Below, we show that if the conditional density estimates can be well estimated, then the conformal adjustment is asymptotically negligible. Thus, a small conformal adjustment may be suggestive of a good conditional density fit and asymptotic conditional coverage rate of  $(1 - \alpha) \times 100\%$  can be obtained. The latter may be established under some regularity conditions, but we shall not pursue this issue here. On the other hand, a large conformal adjustment may signify a bad fit, although the conformal adjustment ensures the  $1 - \alpha$  unconditional coverage rate. Thus, the proposed method preserves the asymptotic  $1 - \alpha$  conditional coverage rate when the underlying conditional density estimation is correctly specified, while guaranteeing  $1 - \alpha$  unconditional coverage, even with an incorrectly specified conditional density estimator. The following regularity conditions will be needed below:

**Assumption 1.** *The sample space of  $(Y, \mathbf{X}^\top)^\top$  is a compact set of the form  $[a, b] \times \mathcal{X}$  where  $a < b$  are two finite numbers, and  $\mathcal{X}$  is a compact subset of the  $d$ -dimensional Euclidean space.*

**Assumption 2.** *The conditional density function  $f(y, \mathbf{x})$  is continuous in  $(y, \mathbf{x})$  and positive, over the sample space.*

**Assumption 3.** *The conditional density estimator  $\hat{f}(\cdot | \mathbf{x})$  converges to  $f(\cdot | \mathbf{x})$  uniformly over the sample space, at the rate of  $b_{n_{train}}$ , in probability, where  $b_{n_{train}} \rightarrow 0$  as the training sample size  $n_{train} \rightarrow \infty$ . That is, there exists a constant  $K$  such that the sup-norm  $\|f(\cdot | \mathbf{x}) - \hat{f}(\cdot | \mathbf{x})\|_\infty \leq K \times b_{n_{train}}$  for all  $\mathbf{x} \in \mathcal{X}$ , except for an event whose probability converges to 0, as  $n_{train} \rightarrow \infty$ . Similarly, the conditional cumulative distribution function  $\hat{F}(\cdot | \mathbf{x})$  converges to  $F(\cdot | \mathbf{x})$  uniformly at the rate of  $b_{n_{train}}$ , in probability.*

**Assumption 4.** *The population quantile function of  $f(Y | \mathbf{X}) - c(\mathbf{X})$  is continuous at  $\alpha$ .*

We remark that assumptions 1 and 2 are mild regularity conditions. The proof of Theorem 2, given in the Supplementary Material, shows that for fixed  $0 < \alpha < 1$ ,  $c(\mathbf{x})$  is a continuous function of  $\mathbf{x}$ , hence assumption 4 holds under very general conditions. Sufficient conditions for assumption 3 have been studied in the literature of kernel density estimation, see Section S4 in the Supplementary Material.

**Theorem 2.** *Suppose assumptions 1–4 hold, and let  $1 > \alpha > 0$  be fixed. Then  $\hat{c}(\mathbf{x})$  converges to  $c(\mathbf{x})$  at the rate of  $b_{n_{train}}$  uniformly in  $\mathbf{x}$ , with probability approaching 1. Moreover, the conformal adjustment  $\hat{q}$ , defined below (1), is of the order  $O_p(b_{n_{train}} + n_{cal}^{-1/2})$ , as both  $n_{cal} \rightarrow \infty$  and  $n_{train} \rightarrow \infty$ .*

The preceding result can be generalized to the case of parametric estimation of the conditional pdf over a possibly non-compact sample space. Assume the true conditional pdf belongs to the model:  $\{f(y | \mathbf{x}; \theta), \theta \in \Theta\}$ , with the parameter estimate from the

training data denoted as  $\hat{\theta} = \hat{\theta}_{train}$ . Write the true cutoff as  $c(\mathbf{x}; \theta)$ , if  $\theta$  were the true parameter. Define  $H(\eta, \mathbf{x}, \theta) = \int_{-\infty}^{\eta} f(y | \mathbf{x}, \theta) dy - \alpha$ . Then,  $c(\mathbf{x}; \theta)$  is the unique solution of  $H(\cdot, \mathbf{x}, \theta) = 0$ . The smoothness property of  $c(\cdot; \cdot)$  can be deduced via the implicit function theorem. The following regularity conditions are mild conditions, e.g., generally satisfied with maximum likelihood estimation of  $\theta$ . Below, denote the true parameter as  $\theta_0$ .

**Assumption 5.** *The estimate  $\hat{\theta} \rightarrow \theta_0$  almost surely. Furthermore,  $f(y | \mathbf{x}; \hat{\theta}) \rightarrow f(y | \mathbf{x}; \theta_0)$  uniformly for  $y, \mathbf{x}$  in any fixed compact set, as  $n_{train} \rightarrow \infty$ .*

**Assumption 6.** *The conditional pdf  $f(y | \mathbf{x}, \theta)$  is a positive, continuous function of  $y, \mathbf{x}, \theta$ . The functions  $\partial H / \partial \mathbf{x} = \int_{-\infty}^{\eta} \partial f(y | \mathbf{x}; \theta) / \partial \mathbf{x} dy$  and  $\partial H / \partial \theta = \int_{-\infty}^{\eta} \partial f(y | \mathbf{x}; \theta) / \partial \theta dy$  are well-defined and continuous functions of  $\eta, \mathbf{x}, \theta$ .*

**Theorem 3.** *Suppose assumptions 4–6 hold, and let  $1 > \alpha > 0$  be fixed. Then  $\hat{c}(\mathbf{x}) = c(\mathbf{x}, \hat{\theta})$  converges to  $c(\mathbf{x}, \theta_0)$  uniformly for  $\mathbf{x}$  in any compact set. Moreover, the conformal adjustment  $\hat{q} \rightarrow 0$ , as both  $n_{cal} \rightarrow \infty$  and  $n_{train} \rightarrow \infty$ .*

## 4 Numerical Studies

In this section, we demonstrate the empirical performance of CHCDS compared to that of HPD-split from Izbicki et al. [2022] in two different scenarios. All analyses were performed using R Statistical Software [R Core Team, 2023]. In both scenarios one predictor was generated,  $X \sim \text{Unif}(-1.5, 1.5)$ . The conditional response setups are below.

Asymmetric:  $Y|X = 5 + 2X + \epsilon|X$ ,  $\epsilon|X \sim \text{Gamma}(\text{Shape} = 1 + 2|X|, \text{Rate} = 1 + 2|X|)$

Mixture:  $Y|X, p \sim p\mathcal{N}\{f(X) - g(X), \sigma^2(X)\} + (1 - p)\mathcal{N}\{f(X) + g(X), \sigma^2(X)\}$ , where  $f(x) = (x-1)^2(x+1)$ ,  $g(x) = 2\mathbb{1}(x \geq -0.5)(x+0.5)^{1/2}$ ,  $\sigma^2(x) = 0.25 + |x|$ , and  $p \sim \text{bin}(0.5)$ .

A scatterplot of the covariate-response relationships can be found in Figure 1. We compared the coverage, average size of the prediction set, and conditional coverage abso-

lute deviation, defined as the absolute difference between the coverage rate,  $1 - \alpha = 0.90$ , and the observed coverage at each value of  $X$ . Simulation standard errors are given in parenthesis if they are larger than 0.001. Unless otherwise stated, all conditional density estimators were fit with Flexcode [Izbicki and Lee, 2017]. We used a Fourier basis and the regression functions were estimated with Nadaraya Watson Regression. We also looked at how well a conditional kernel density estimator (Kernel), a conditional kernel density estimator computed only on the 75 nearest neighbors of  $\mathbf{X}_i$  (KNN Kernel), and a Gaussian mixture distribution with four components for the joint density and two components for the marginal covariate density (Gaussian Mix) performed in both scenarios using CHCDS, see Section S3 in the Supplementary Material for details. All simulations had a simulation size of 10,000. Each scenario had 1,000 training samples and 500 calibration samples. Results can be found in Table 1 and Table 2. Monte Carlo error is given in parentheses only if it is greater than 1. All values have been multiplied by  $10^3$ . Graphical comparisons of conditional coverage can be found in Figure 2. Unadjusted represent the unadjusted highest density set that was estimated using the conditional density estimator without any conformal adjustments. Plots showing examples of the prediction regions can be found in the Supplementary Material (Figure S7 – Figure S18.)

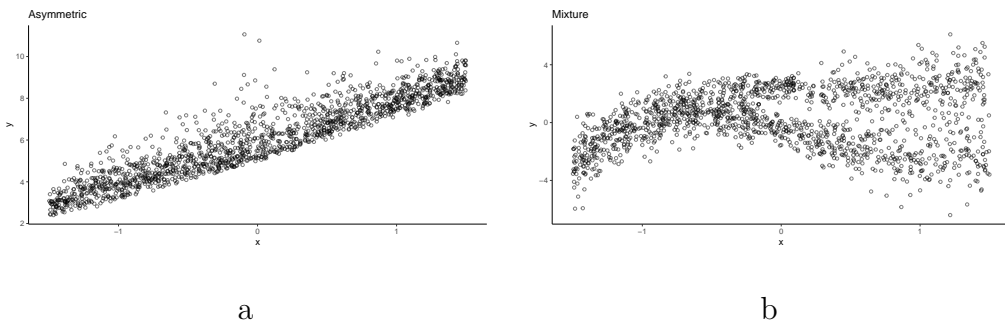


Figure 1: Left diagram: a plot showing the covariate response relationship from one simulation in the asymmetric scenario. Right diagram is that in the mixture scenario.

It is clear from the simulations that CHCDS and HPD-split give very similar results



Table 1: Comparison of the methods in the asymmetric scenario

Approach	Coverage	Size	Conditional Absolute Deviation
Unadjusted (FlexCode)	969 (2)	4054 (2)	74 (1)
HPD-split (FlexCode)	908 (3)	2307 (2)	30 (1)
CHCDS (FlexCode)	907 (3)	2253 (2)	29 (1)
CHCDS (Kernel)	900 (3)	1957 (1)	14
CHCDS (KNN)	900 (3)	1944 (1)	12
CHCDS (Gaussian Mix)	902 (3)	2005 (2)	30 (1)

Table 2: Comparison of the methods in the mixture scenario

Approach	Coverage	Set Size	Conditional Absolute Deviation
Unadjusted (FlexCode)	925 (3)	5878 (2)	58 (1)
HPD-split (FlexCode)	900 (3)	5466 (3)	63 (1)
CHCDS (FlexCode)	904 (3)	5526 (3)	64 (1)
CHCDS (Kernel)	904 (3)	5668 (3)	79 (1)
CHCDS (KNN)	906 (3)	5319 (2)	8
CHCDS (Gaussian Mix)	903 (3)	5156 (2)	28 (1)

when the same density estimator is used. In both methods, we can also see that without a conformal adjustment, the prediction sets are needlessly large and have poor nominal coverage. As expected, the results heavily depend on how good the initial density estimator is. One advantage of CHCDS compared to HPD-split is how easy it is to use density estimators other than those found in Izbicki and Lee [2017]. When looking at conditional mixture distributions, we can use a density estimator that weights nearby points more heavily. This is clearly an advantage of CHCDS with the KNN conditional kernel density estimator in Figure 2b compared to HPD-split. The KNN conditional kernel density es-

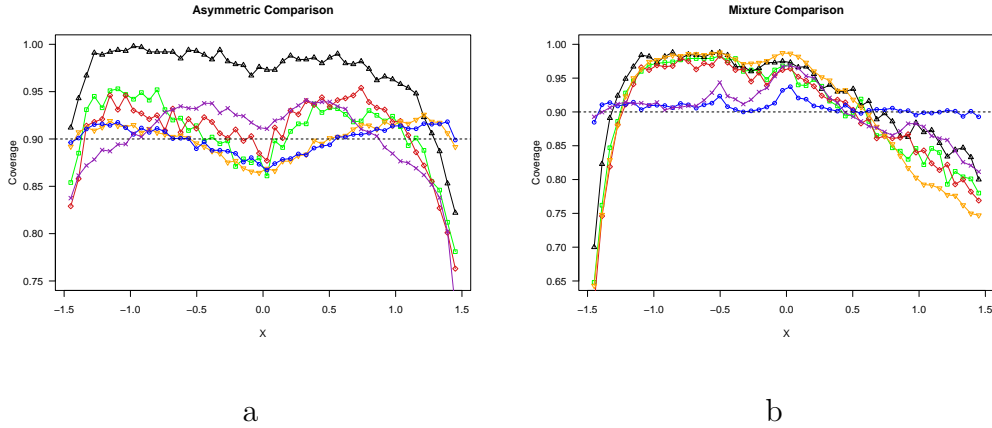


Figure 2: Left (right) diagram showing the comparison of conditional coverage in the asymmetric (mixture) scenario between unadjusted FlexCode (black triangles), HPD-split (red diamonds), CHCDS FlexCode (green squares), CHCDS Kernel (orange nablas), CHCDS KNN (blue circles), and CHCDS Gaussian Mixture (purple X). The dashed line represents the desired 90% coverage. The other lines represent the conditional coverage at a given value of  $X$ .

timator with a CHCDS adjustment has nearly perfect conditional 90% coverage. All the other methods under cover in the tails. See Section S6 in the Supplementary Material for further discussion.

## 5 Real Data Analysis

We used a Gaussian mixture density estimator with four mixture components for the joint density and three for the marginal covariate density on the HappyA dataset, which contains 74,950 galaxies [Beck et al., 2017]. We used the *densityMclust* function from the *mclust* package to build the model [Scrucca et al., 2023]. See Section S7 in the Supplementary Material for an alternative implementation of the mixture model fitting, via neural network, which provided slightly better performance. Our goal was to predict galaxy red-

shift based on r-magnitude and the brightness of 4 non-red colors. It is known that the conditional density of redshift can be multimodal [Sheldon et al., 2012, Izbicki et al., 2022, Carrasco Kind and Brunner, 2013]. We used 64,950 observations to train the model, 5,000 to compute non-conformity scores, and 5,000 to test out of sample prediction. This was repeated 10 times. We only compared unadjusted FlexCode, HPD-split, CHCDS-FlexCode, and CHCDS-Gaussian Mix because the kernel methods were unable to handle the 7 dimensional data. For all of the FlexCode methods, we used 15,000 observations to train the model, 1,000 for calibration, and 1,000 for out of sample test predictions because using all of the data was not computationally feasible for the FlexCode density estimators. Our goal was to create prediction sets with a coverage rate of 90%. We also looked at the conditional coverage for bright and faint galaxies. We defined bright galaxies as those with an r-magnitude less than the median, 19.22, and faint as those with an r-magnitude greater than the median. The results can be found in Table 3 and Table 4. Standard errors are given in parentheses if they are greater than 1. All values have been multiplied by  $10^3$ .

Table 3: Coverage and average size of the prediction regions for each method.

Type	Coverage	Size
Unadjusted (FlexCode)	966	465 (1)
HPD-split (FlexCode)	905	301 (1)
CHCDS (FlexCode)	905	283 (1)
CHCDS (Gaussian Mix)	900	149

We can see from the results that none of the FlexCode density estimators performed very well. The best estimator in this analysis was the conditional Gaussian mixture density estimator. The flexibility provided by CHCDS allowed us to use the best estimator for the problem, instead of being stuck with a poorly performing model. Both Gaussian mixture density estimators were also able to use all of the available data because storing

Table 4: Conditional coverage and average size of the prediction regions for bright and faint galaxies.

Type	Bright Coverage	Bright Size	Faint Coverage	Faint Size
Unadjusted (FlexCode)	993	456 (1)	938	474 (1)
HPD-split (FlexCode)	952	305 (1)	859	297 (1)
CHCDS (FlexCode)	925	248 (1)	886	317 (1)
CHCDS (Gaussian Mix)	904	95	895	204

the parameters did not require a large amount of memory, compared to the large number of regression models needed to be stored for FlexCode.

## 6 Discussion

From the numerical results, it is clear the main advantage of CHCDS is that it can be quickly used with any existing conditional density estimation method. Because there are existing packages that can find the initial  $1 - \alpha$  prediction set, for instance, the R package *hdrcde* and the python packages for normalizing flows and many mixture density network [Rothfuss et al., 2019] with the initial set being found using the *hdi* function from the *arviz* library [Kumar et al., 2019], CHCDS can be applied in multiple languages using many out of the box estimators.

The major drawback of CHCDS is similar to the drawbacks of other conformal prediction methods, in that its performance hinges on that of the model. Moreover, the prediction set may not be a connected region which may make interpretation hard. Though, an image of the conditional density can help understanding.

## Acknowledgement

This project was partially funded by National Institutes of Health Predoctoral Training Grant T32 HL 144461.

# Supplementary material for Flexible Conformal Highest Predictive Conditional Density Sets

## S1 Conformal Prediction

Conformal prediction is a general method of creating prediction intervals that provide a non-asymptotic, distribution free coverage guarantee. Suppose we observe  $n$  i.i.d. (more generally, exchangeable) copies of  $\{(Y_1, \mathbf{X}_1), (Y_2, \mathbf{X}_2), \dots, (Y_n, \mathbf{X}_n)\}$ , with distribution  $P$ . Suppose that the first  $n$  pairs are observed. Then, we want a set,  $C(\mathbf{x}) = C_n((Y_1, \mathbf{X}_1), (Y_2, \mathbf{X}_2), \dots, (Y_n, \mathbf{X}_n), \mathbf{x})$  such that for a new pair  $(Y_{n+1}, \mathbf{X}_{n+1})$ ,

$$pr\{Y_{n+1} \in C(\mathbf{X}_{n+1})\} \geq 1 - \alpha \quad (\text{S1})$$

This coverage is guaranteed unconditionally [Vovk et al., 2005, Lei and Wasserman, 2012]. If we wanted to have finite sample, distribution-free, and conditional coverage for a continuous response,

$$pr\{Y_{n+1} \in C(\mathbf{X}_{n+1}) \mid \mathbf{X}_{n+1}\} \geq 1 - \alpha, \quad a.s. \quad (\text{S2})$$

our expected prediction set length would be infinite [Lei and Wasserman, 2012].

A method that attempts to approximate conditional coverage is locally valid conditional coverage. Let  $\mathcal{A} = \{A_j : j \geq 1\}$  be a partition of the covariate space. A prediction set,  $C(\mathbf{x})$  is locally valid with respect to  $\mathcal{A}$  if

$$pr\{Y_{n+1} \in C(\mathbf{X}_{n+1}) \mid \mathbf{X}_{n+1} \in A_j\} \geq 1 - \alpha, \text{ for all } j.$$

Local validity is achieved by computing conformal prediction sets using only the data within each partition. These sets tend to involve partitions of the data where prediction sets are formed based on density estimators within each partition [Izbicki et al., 2020, 2022, Lei and Wasserman, 2014]. When non-conformity score are almost surely distinct, the coverage probability when conditioning on both the training and calibration sets is a

random quantity,

$$\mathbb{P}(Y_{n+1} \in C(\mathbf{X}_{n+1}) \mid (\mathbf{X}_i, Y_i), i = 1, \dots, n) \sim \text{Beta}(\kappa_\alpha, n_{cal} + 1 - \kappa_\alpha),$$

where  $\kappa_\alpha = \lceil (1 - \alpha)(n_{cal} + 1) \rceil$  [Vovk, 2012, Angelopoulos and Bates, 2021]. The idea is, if we run the conformal prediction algorithm multiple times, each time sampling a new finite observed dataset, then check the coverage on an infinite number of validation points, each coverage rate will be a draw from the above Beta distribution. So, when using partitions our prediction sets have more variability in coverage conditional on the observed data because we have a smaller sample size within each partition than we do overall [Lei and Wasserman, 2014, Izbicki et al., 2022, Angelopoulos and Bates, 2021].

For completion, we include an outline of the HPD-split method in Algorithm 2. The score used in HPD-split can be seen visually in Figure S1.

---

**Algorithm 2** HPD-Split

---

**Input:** level  $\alpha$ , data  $= \mathcal{Z} = (Y_i, \mathbf{X}_i)_{i \in \mathcal{I}}$ , test point  $(\mathbf{x})$ , and conditional density algorithm

$\mathcal{B}$

**Procedure:**

- 1: Split  $\mathcal{Z}$  into a training fold  $\mathcal{Z}_{tr} \triangleq (Y_i, \mathbf{X}_i)_{i \in \mathcal{I}_{tr}}$  and a calibration fold  $\mathcal{Z}_{cal} \triangleq (Y_i, \mathbf{X}_i)_{i \in \mathcal{I}_{cal}}$
  - 2: Fit  $\hat{f} = \mathcal{B}(\{(\mathbf{X}_i, Y_i) : i \in \mathcal{I}_{tr}\})$
  - 3: Let  $\hat{H}$  be an estimate of the cdf of the split residuals,  $\hat{f}(Y|\mathbf{X})$ , obtained by numerical integration
  - 4: Let  $U_{[\alpha]}$  be the  $\lfloor \alpha(n_{cal} + 1) \rfloor$  smallest value of  $\{\hat{H}(\hat{f}(y_i|\mathbf{x}_i)|\mathbf{x}_i) : i \in \mathcal{I}_{cal}\}$
  - 5: Build a finite grid over  $\mathcal{Y}$  and, by interpolation, **return**  $\{y : \hat{H}(\hat{f}(y|\mathbf{x})|\mathbf{x}) \geq U_{[\alpha]}\}$
- 

A visual of how the CHCDS score works can be seen in Figure S2. The main advantages of CHCDS compared to other methods is that it does not partition the data and that it can easily be used with any existing conditional density estimator.

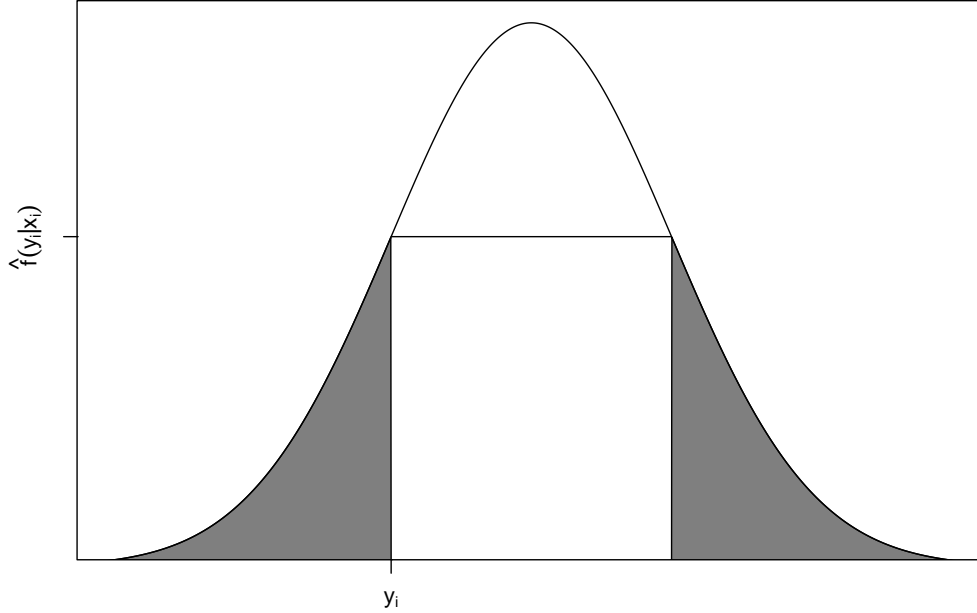


Figure S1: The HPD-split score for a sample  $(y_i, \mathbf{x}_i)$  is the shaded region of the plot.

## S2 CHCDS Comparison

A problem can occur when the prediction level is high and the conditional density estimator overestimates the estimated density value cutoff for the unadjusted  $1 - \alpha$  prediction set (that is, the estimated density under covers before the conformal adjustment). When this occurs, the final density cutoff for the new prediction point is a negative value, or an infinite prediction set. To solve this issue, we propose a new method below that has the same properties and benefits as CHCDS without this potential drawback.

Let the new conformity scores be

$$V_i = \hat{f}(Y_i | \mathbf{X}_i) / \hat{c}(\mathbf{X}_i), \forall i \in \mathcal{I}_{cal}.$$

Then, the final conformal prediction set will be

$$\mathbf{C}(\mathbf{X}_{n+1}) = \{y : \hat{f}(y | \mathbf{X}_{n+1}) > \hat{c}(\mathbf{X}_{n+1}) \times \hat{q}\},$$



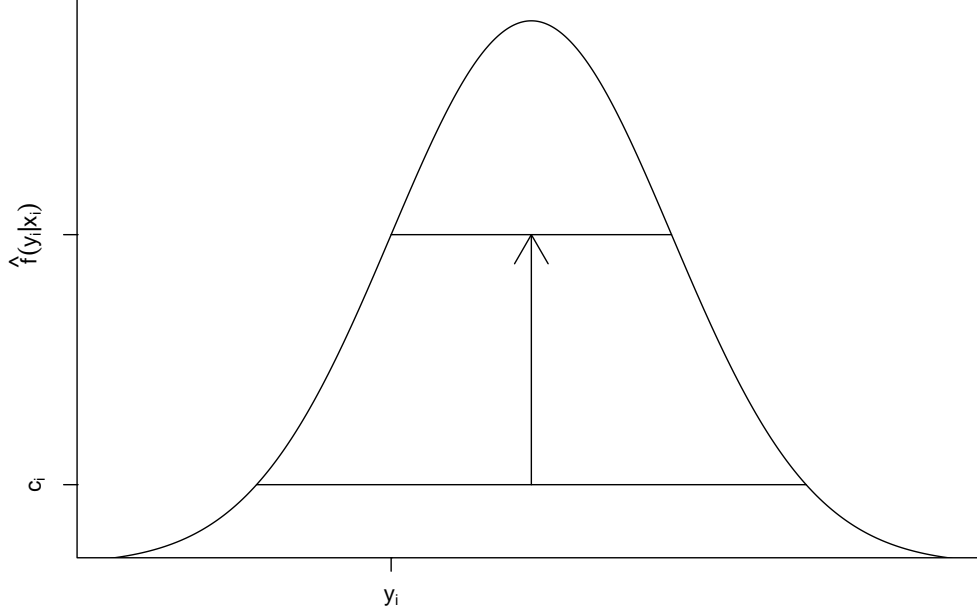


Figure S2: The CHCDS score for a sample  $(y_i, \mathbf{x}_i)$  is shown by the arrow.

where  $\hat{q} = \lfloor \alpha(n_{cal} + 1) \rfloor$ th smallest value of  $\{\mathbf{V}\}$ . When the conditional density has a high variability, so the density cutoff values are small, we can add a small constant,  $\gamma$  for numerical stability.

$$V_i = \hat{f}(Y_i | \mathbf{X}_i) / (\hat{c}(\mathbf{X}_i) + \gamma), \forall i \in \mathcal{I}_{cal}.$$

Then, the final conformal prediction set will be

$$\hat{\mathbf{C}}(\mathbf{X}_{n+1}) = \{y : \hat{f}(y | \mathbf{X}_{n+1}) > (\hat{c}(\mathbf{X}_{n+1}) + \gamma) \times \hat{q}\},$$

where  $\hat{q} = \lfloor \alpha(n_{cal} + 1) \rfloor$ th smallest value of  $\{\mathbf{V}\}$ .

We include a comparison of CHCDS-subtraction with this method for some of the simulation scenarios. The results in all cases are nearly identical. We also include a toy simulation example to demonstrate how CHCDS can cause infinite prediction sets.

Below are two plots comparing additive conformal adjustment versus multiplicative conformal adjustment, referred to as CHCDS-subtraction and CHCDS-division, with different density estimators in the mixture scenario with the same simulation size and sample sizes as in Section 4. We set the coverage rate to be  $1 - \alpha = 99\%$  to see how well both methods performed in an edge case. In Figure S3 and Figure S4 the blue line is the conditional coverage for CHCDS-subtraction and the black line is the conditional coverage for CHCDS-division. In this scenario, we can see they are nearly identical. In both cases, the subtraction method did not output an infinite prediction set.

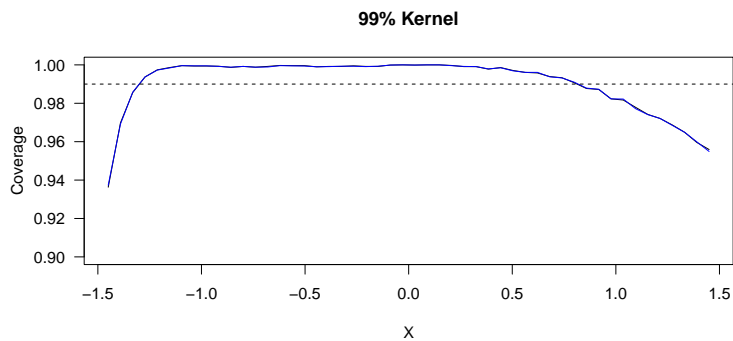


Figure S3: Comparison of conditional coverage between CHCDS-subtraction Kernel (blue) and CHCDS-division Kernel (black) in the mixture scenario. The dashed line shows the desired 99% coverage.

To show the potential failure of CHCDS-subtraction, we looked at a heteroskedastic example with data generated in the following way.  $X \sim \text{Unif}(-5, 5)$ ,  $Y | X \sim \mathcal{N}(0, |X| + 0.01)$ . A scatterplot of the relationship between the response and covariate can be found in Figure S5. Data were split, 1000 for training and 500 for calibration. The simulation size was 10,000. We only used a conditional kernel density estimator. The target coverage rate was  $1 - \alpha = 99\%$ , but we found the 98.5% unconformalized estimated highest density cut-off. This, along with the heteroskedastic nature of the data, was to ensure we would need to lower the cut-off with our conformal adjustment, while having high variability conditional densities (and, thus, density cut-off values near 0). The comparison of the

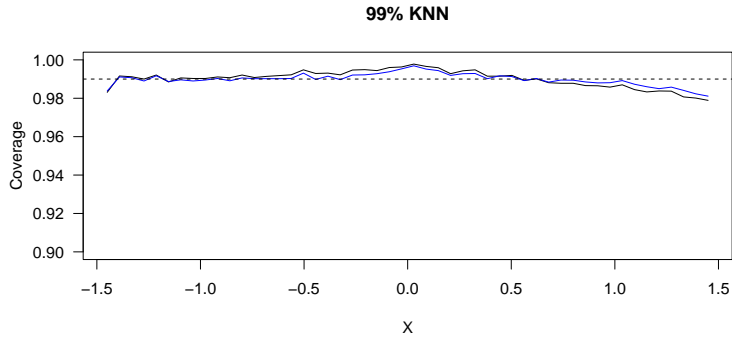


Figure S4: Comparison of conditional coverage between CHCDS-subtraction (KNN) (blue) and CHCDS-division (KNN) (black) in the mixture scenario. The dashed line shows the desired 99% coverage.

method's conditional coverages can be found in Figure S6. CHCDS-subtraction gave infinite prediction intervals in 1.13% of the out of sample test cases. As expected, these nearly all occurred in the regions with large variability, which correspond to large values of  $|X|$ . CHCDS-division never gave an infinite prediction interval.

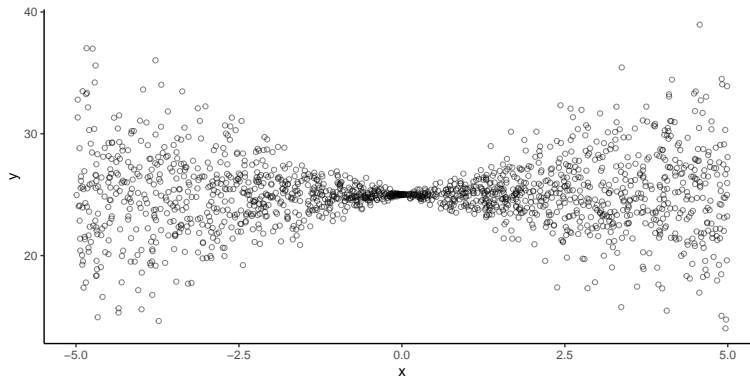


Figure S5: A scatterplot of the heteroskedastic Normal distribution response covariate relationship.

### S3 Conditional Density Estimation

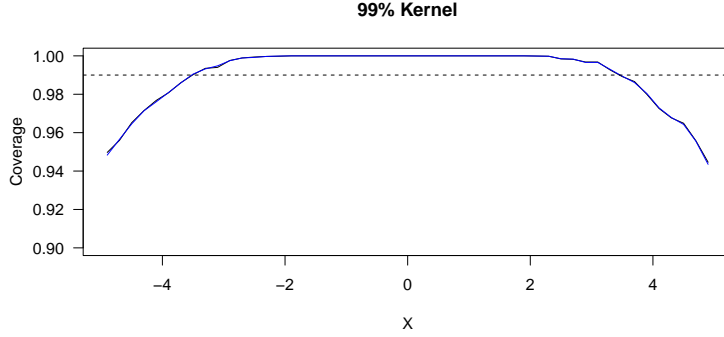


Figure S6: Comparison of conditional coverage between CHCDS-subtraction Kernel (blue) and CHCDS-division Kernel (black) in the heteroskedastic Normal scenario. The dashed line shows the desired 99% coverage.

In this section, we describe some existing methods for conditional density estimation. Denote the conditional density estimator as  $\hat{f}(Y | \mathbf{X})$ , where  $\mathbf{X}$  are the  $d$  conditioning variables. The simplest method for conditional density estimation comes from Hirano and Imbens [2004], where they used it to estimate generalized propensity scores. They assumed that

$$Y | \mathbf{X} \sim \mathcal{N}\{\mu(\mathbf{X}), \sigma^2\}.$$

They then estimated the function  $\mu$  and  $\sigma^2$  with  $\hat{\mu}$  and  $\hat{\sigma}^2$  using least squares regression. Using these estimations, the conditional densities were computed as

$$\hat{f}(y | \mathbf{X}) = (2\pi\hat{\sigma}^2)^{-1/2} \exp[-\{y - \hat{\mu}(\mathbf{X})\}^2 / (2\hat{\sigma}^2)].$$

A non-parametric approach to density estimation is kernel density estimation. It was originally a form of unconditional density estimation [Rosenblatt, 1956, Parzen, 1962]. Let  $K(y)$  be the kernel function chosen. Assume that  $K(y)$  is symmetric,  $\int_{-\infty}^{\infty} y^2 K(y) dy < \infty$ , and  $\int_{-\infty}^{\infty} K(y) dy = 1$ . Denote  $h$  as the bandwidth, or smoothing parameter, of the chosen kernel density estimator such that  $h \rightarrow 0$  and  $nh \rightarrow \infty$  as  $n \rightarrow \infty$ . The bandwidth  $h$  is

commonly chosen to be a function of  $n$ . Then, the kernel density estimator is

$$\hat{f}(y) = (nh)^{-1} \sum_{i=1}^n K\{(Y_i - y)/h\}.$$

Hyndman et al. [1996] extended this idea to kernel conditional density estimation. Let  $f(y, \mathbf{x})$  denote the joint density of  $(Y, \mathbf{X})$  and  $f(\mathbf{x})$  denote the marginal density of  $\mathbf{X}$ . Then, we can write the conditional density of  $Y \mid (\mathbf{X} = \mathbf{x})$  as  $f(y \mid \mathbf{x}) = f(y, \mathbf{x})/f(\mathbf{x})$ . The kernel conditional density estimator is then

$$\hat{f}(y \mid \mathbf{x}) = \hat{f}(y, \mathbf{x})/\hat{f}(\mathbf{x}), \tag{S3}$$

where

$$\hat{f}(y, \mathbf{x}) = (n \times b \times \prod_{i=1}^n a_i)^{-1} \sum_{j=1}^n K(b^{-1} \|y - Y_j\|_y) \times \prod_{i=1}^d K(a_i^{-1} \|x_i - X_{ij}\|_x)$$

and

$$\hat{f}(\mathbf{x}) = (n \times \prod_{i=1}^n a_i)^{-1} \sum_{j=1}^n \prod_{i=1}^d K(a_i^{-1} \|x_i - X_{ij}\|_x),$$

where  $\mathbf{X}_i = (X_{i1}, \dots, X_{id})^\top$ . Here,  $\|\cdot\|_x$  and  $\|\cdot\|_y$  are distance metrics, for example the Euclidean distance. The kernel used satisfies the same properties as those used in unconditional kernel density estimation, and  $a_i$  and  $b$  are the bandwidth parameters [Rosenblatt, 1971, Cacoullos, 1966], which are often taken to be identically equal to  $h$  if the variables are of similar scale.

Kernel density estimation gives more influence to points closer to the point of interest, but that influence can be increased by computing the density estimates on the nearest  $k$  neighbors, instead of on all  $n$  data points. This can work well if we have a large number of data points and the true conditional density varies heavily depending on the covariates, for example a mixture distribution [Izbicki et al., 2019]. Instead of a vector for the covariate's bandwidth, a bandwidth matrix along with a multivariate kernel can be used [Mack and Rosenblatt, 1979].

Another combination of k-nearest neighbors and kernel density estimation replaces the bandwidths,  $h$ ,  $a$ , and  $b$ , with the distance from the  $k$ th nearest neighbor to  $\mathbf{x}$  or  $y$  [Mack

and Rosenblatt, 1979, Moore and Yackel, 1977, Loftsgaarden and Quesenberry, 1965]. This allows for unequal weighting of the observations. There are many other ways of choosing kernel density bandwidths and automatically selecting bandwidths that can be found in Chiu [1996], Heidenreich et al. [2013].

FlexCode is another non-parametric density estimator. First, the response is scaled to be in the interval  $[0, 1]$ . Then, FlexCode uses a basis expansion to model the density. One option for the basis is the Fourier basis:

$$\phi_1(z) = 1; \quad \phi_{2i+1}(z) = 2^{1/2} \sin(2\pi iz) \quad \phi_{2i}(z) = 2^{1/2} \cos(2\pi iz), \quad i \in \mathbb{N}.$$

For a fixed  $\mathbf{x}$ , as long as  $\int_{-\infty}^{\infty} |f(y | \mathbf{x})|^2 dy < \infty$ , the conditional density can be written as

$$f(y | \mathbf{x}) = \sum_{i \in \mathbb{N}} \beta_i(\mathbf{x}) \phi_i(y),$$

where  $\beta_i(\mathbf{x}) = \mathbb{E}(\phi_i(Y) | \mathbf{x})$  [Izbicki and Lee, 2016]. Now, define the FlexCode conditional density estimator as

$$\hat{f}(y | \mathbf{x}) = \sum_{i=1}^I \hat{\beta}_i(\mathbf{x}) \phi_i(y),$$

where  $\hat{\beta}_i(\mathbf{x})$  is estimated using a conditional mean algorithm (for example, a random forest estimator) and  $I$  is a tuning parameter that controls the bias-variance tradeoff [Izbicki and Lee, 2017].

Mixture models are a parametric approach to finding an estimate of the conditional density [Bishop, 1994]. Let the joint density be represented as

$$f_{\boldsymbol{\theta}}(y, \mathbf{x}) = \sum_{i=1}^K \pi_i f_{\boldsymbol{\psi}_i}(y, \mathbf{x}),$$

where  $K$  represents the number of mixture components,  $\pi_j$  represents the weight of the  $j$ th mixture component, and  $\boldsymbol{\psi}_j$  represents the parameters of the  $j$ th mixture component. For example, the mean vector and covariance matrix for a Normal distribution [Chassagnol et al., 2023]. These parameters can be estimated using an iterative process, for example an EM algorithm or a deep neural network [Viroli and McLachlan, 2019].

We can use the same idea to estimate the marginal density of  $\mathbf{X}$ ,

$$g_{\zeta}(\mathbf{x}) = \sum_{i=1}^J \pi_i g_{\eta_i},$$

where  $J$  represents the number of mixture components,  $\pi_j$  represents the weight of the  $j$ th mixture component, and  $\boldsymbol{\eta}_j$  represents the parameters of the  $j$ th mixture component. Combining the joint and marginal estimates, the conditional mixture density estimator is

$$\hat{f}(y | \mathbf{x}) = f_{\hat{\boldsymbol{\theta}}}(y, \mathbf{x}) / g_{\hat{\zeta}}(\mathbf{x}).$$

A second approach to conditional density estimation with mixture distributions is to assume that the conditional distribution of  $Y | \mathbf{X}$  is the convolution of  $K$  distributions.

$$f_{\boldsymbol{\theta}}(y | \mathbf{x}) = \sum_{i=1}^K \pi_i f_{\boldsymbol{\psi}_i}(y | \mathbf{x}),$$

where  $K$  represents the number of mixture components,  $\pi_j$  represents the weight of the  $j$ th mixture component, and  $\boldsymbol{\psi}_j$  represents the parameters of the  $j$ th mixture component. Though the true density may not be a mixture of, for example, Normal distributions, a Gaussian mixture distribution can provide a reasonable approximation.

Normalizing flows are another method that can be used for conditional density estimation. Start with the idea of a change of variable transformation. Let  $y = g(u)$ , where  $g$  is a bijective and differentiable function and  $\pi(\cdot)$  is the density of  $U$ . The density of  $Y$  can then be represented as

$$f_Y(y) = \pi\{g^{-1}(y)\} \left| \det \frac{\partial g^{-1}}{\partial y}(y) \right|.$$

The base density, which is typically chosen to be easy to evaluate for any input (a common choice is a standard Gaussian density) [Papamakarios et al., 2017].

Extending this idea to a conditional distribution is fairly straightforward. Let  $y = g(u, \mathbf{x})$ , where  $g$  is a bijective and differentiable function and  $\pi(\cdot | \mathbf{x})$  is the conditional density of  $U | \mathbf{x}$ . The conditional density of  $Y | \mathbf{x}$  can then be represented as

$$f_{Y|\mathbf{X}}(y | \mathbf{x}) = \pi\{g^{-1}(y, \mathbf{x}) | \mathbf{x}\} \left| \det \frac{\partial g^{-1}}{\partial y}(y, \mathbf{x}) \right|.$$

As in the unconditional case, the base density is typically chosen to be easy to evaluate [Winkler et al., 2023]. For example, we might have  $U \mid X \sim \mathcal{N}(0, |X|^2)$  and  $Y \mid X \sim \mathcal{N}(X, |X|^2)$ . Then our function,  $g(u, x) = u + x = y$ ,  $g^{-1}(y, x) = y - x$ , and  $|\partial g^{-1}(y, x)/\partial y| = 1$  [Kingma et al., 2016].

When doing conditional density estimation, we typically do not know what the function  $g$  is, or even if we can find a suitable transformation using only one function. Instead, let  $y = g_K(g_{K-1}(\dots g_1(u_0, x)))$ . The log-likelihood for  $f_{Y|\mathbf{x}}(y, \mathbf{x})$  can then be written as

$$f_{Y|\mathbf{x}}(y, \mathbf{x}) = \log\{\pi(u_0 \mid \mathbf{x})\} - \sum_{i=1}^K \log \left\{ \left| \det \frac{\partial g_i}{\partial u_{i-1}}(u_{i-1}, \mathbf{x}) \right| \right\}, \quad (\text{S4})$$

where  $u_i = g_i(u_{i-1}, \mathbf{x})$  [Trippe and Turner, 2018, Rezende and Mohamed, 2015]. Knowing this gives us a function to maximize, so the negative of (S4) becomes our objective loss function. The functions,  $g$ , typically have parameters that need to be estimated. In the earlier example of  $g(u, x) = u + x$ , the function might actually be  $g(u, x) = u + \mu(x)$ , where we do not know  $\mu(\cdot)$ . [Papamakarios et al., 2017, Winkler et al., 2023]. We can use neural networks (or other tools) along with (S4) to approximate the  $g$  functions. Combining these estimates gives us an estimate for  $\hat{f}_{Y|\mathbf{x}}(y \mid \mathbf{x})$ . There are many classes of  $g$ 's that can be used in normalizing flows, see Winkler et al. [2023], Trippe and Turner [2018], Kobayev et al. [2021], Papamakarios et al. [2021] for examples.

## S4 Sufficient conditions for assumption 3

The validity of assumption 3 requires technical conditions on both the true density function and the kernel function. Given assumptions 1 and 2, and that the joint pdf  $f(y, \mathbf{x})$  is  $\zeta$ -Hölder continuous, where  $0 < \zeta \leq 1$ , (i.e., there exists a constant  $K'$  such that  $|f(y, \mathbf{x}) - f(y', \mathbf{x}')| \leq K'(|y - y'| + |\mathbf{x} - \mathbf{x}'|)^\zeta$  for all  $(y, \mathbf{x})$  and  $(y', \mathbf{x}')$ ). Consider kernel density estimation defined by (S3) with a spherically symmetric kernel of compact support, using Euclidean distance and with identical bandwidth equal to  $h$ . Let



$b_n = h^\zeta + \{\log n / (nh^{d+1})\}^{1/2}$ . Suppose  $h > (\log n/n)^{1/(d+1)}$  and  $h \rightarrow 0$  as  $n \rightarrow \infty$ . Under the preceding conditions, [Jiang, 2017, Theorem 2] implies the validity of assumption 3. This is because it follows from [Jiang, 2017, Theorem 2] that  $|\hat{f}(y, \mathbf{x}) - f(y, \mathbf{x})|$  is less than a fixed multiple of  $b_n$  for all  $\mathbf{x}$ , except for an event of probability less than  $1/n$ , and the same holds for  $|f(\mathbf{x}) - \hat{f}(\mathbf{x})|$ . The convergence regarding  $\hat{f}(\cdot | \mathbf{x})$ , as stated in assumption 3, then follows from the inequality

$$\begin{aligned} & |\hat{f}(y | \mathbf{x}) - f(y | \mathbf{x})| \\ & \leq \{|\hat{f}(y, \mathbf{x}) - f(y, \mathbf{x})| + f(y | \mathbf{x})|f(\mathbf{x}) - \hat{f}(\mathbf{x})|\} / \hat{f}(\mathbf{x}). \end{aligned}$$

Note that for all sufficiently small  $h$ , the support of the kernel density estimator  $\hat{f}(y, \mathbf{x})$  lies within some fixed compact set, hence the claim concerning the uniform convergence of  $\hat{F}(\cdot | x)$  can be readily verified.

## S5 Proofs

The next two lemmas come from Romano et al. [2019], Tibshirani et al. [2019], Lei et al. [2018], Vovk et al. [2005].

**Lemma 1.** (*Quantiles and exchangeability*). *Suppose  $Z_1, \dots, Z_n$  are exchangeable random variables.*

*For any  $\alpha \in (0, 1)$ ,*

$$\text{pr}\{(Z_n \leq \hat{R}_n(\alpha))\} \geq \alpha,$$

*where  $\hat{R}_n$  is the empirical quantile function,  $\hat{R}_n(\alpha) = Z_{(\lceil \alpha n \rceil)}$ .*

*Moreover, if the random variables  $Z_1, \dots, Z_n$  are almost surely distinct, then*

$$\text{pr}\{Z_n \leq \hat{R}_n(\alpha)\} \leq \alpha + \frac{1}{n}.$$

**Lemma 2.** (*Inflation of Quantiles*). Suppose  $Z_1, \dots, Z_n$  are exchangeable random variables.

For any  $\alpha \in (0, 1)$ ,

$$\text{pr}\{Z_{n+1} \leq \hat{R}_n\{(1 + n^{-1})\alpha\}\} \geq \alpha.$$

Moreover, if the random variables  $Z_1, \dots, Z_n$  are almost surely distinct, then

$$\text{pr}\{Z_{n+1} \leq \hat{R}_n\{(1 + n^{-1})\alpha\}\} \leq \alpha + (n + 1)^{-1}.$$

The following two lemmas are similar to those from Romano et al. [2019], Tibshirani et al. [2019], Lei et al. [2018], Vovk et al. [2005], but we look at the set formed by finding values of  $y$  that make the score greater than a cutoff instead of less than or equal to a cutoff.

**Lemma 3.** Suppose  $Z_1, \dots, Z_n$  are exchangeable random variables.

For any  $\alpha \in (0, 1)$ ,

$$\text{pr}\{Z_n > \hat{Q}_n(\alpha)\} \geq 1 - \alpha,$$

where  $\hat{Q}_n$  is the empirical quantile function,  $\hat{Q}_n(\alpha) = Z_{(\lfloor \alpha n \rfloor)}$ . Moreover, if the random variables  $Z_1, \dots, Z_n$  are almost surely distinct, then

$$\text{pr}\{Z_n > \hat{Q}_n(\alpha)\} \leq 1 - \alpha + n^{-1}.$$

*Proof.* For the lower-bound, by exchangeability of  $Z_1, \dots, Z_n$ ,  $\text{pr}\{Z_i > \hat{Q}_n(\alpha)\} = \text{pr}\{Z_n > \hat{Q}_n(\alpha)\}$ , for all  $i$ . Therefore,

$$E[1 - \hat{F}_n\{\hat{Q}_n(\alpha)\}] = \sum_{i=1}^n n^{-1} \text{pr}\{Z_i > \hat{Q}_n(\alpha)\} = \text{pr}\{Z_n > \hat{Q}_n(\alpha)\},$$

where  $\hat{F}_n(z) := n^{-1} \sum_{i=1}^n \mathbb{1}(Z_i \leq z)$ .

By the definition of the empirical cdf,  $1 - \hat{F}_n\{\hat{Q}_n(\alpha)\} \geq 1 - \alpha$ .

Taking the expectation, we get,

$$\text{pr}\{Z_n > \hat{Q}_n(\alpha)\} \geq 1 - \alpha,$$

as desired.

For the upper-bound, apply Lemma 1 with  $\hat{R}_n(\alpha) = Z_{(\lceil \alpha n - 1 \rceil)}$  instead of  $Z_{(\lceil \alpha n \rceil)}$ . Then we have that

$$\alpha - n^{-1} \leq \text{pr}\{Z_n \leq Z_{(\lceil \alpha n - 1 \rceil)}\}.$$

Notice that  $Z_{(\lceil \alpha n - 1 \rceil)} \leq Z_{(\lfloor \alpha n \rfloor)}$ , so

$$1 - (\alpha - n^{-1}) \geq \text{pr}\{Z_n > Z_{(\lceil \alpha n - 1 \rceil)}\} \geq \text{pr}\{Z_n > \hat{Q}_n(\alpha)\}.$$

So,

$$1 - \alpha + n^{-1} \geq \text{pr}\{Z_n > \hat{Q}_n(\alpha)\}.$$

□

**Lemma 4.** *Suppose  $Z_1, \dots, Z_n$  are exchangeable random variables.*

*For any  $\alpha \in (0, 1)$ ,*

$$\text{pr}[Z_{n+1} > \hat{Q}_n\{(1 + n^{-1})\alpha\}] \geq 1 - \alpha.$$

*Proof.* Let  $Z_{(k,m)}$  denote the  $k$ th smallest value in  $Z_1, \dots, Z_m$ .

For any  $0 \leq k \leq n$ , we have

$$Z_{n+1} > Z_{(k,n)} \text{ if and only if } Z_{n+1} > Z_{(k,n+1)}$$

First, assume  $Z_{n+1} > Z_{(k,n)}$ , then  $Z_{(k,n+1)} = Z_{(k,n)}$ , so  $Z_{n+1} > Z_{(k,n+1)}$ .

Second, assume  $Z_{n+1} > Z_{(k,n+1)}$ , then  $Z_{(k,n)} = Z_{(k,n+1)}$ , so  $Z_{n+1} > Z_{(k,n)}$ .

Now, because  $\hat{Q}_n\{(1 + n^{-1})\alpha\} = Z_{(\lfloor \alpha(n+1) \rfloor, n)}$  and  $\hat{Q}_{n+1}(\alpha) = Z_{(\lfloor \alpha(n+1) \rfloor, n+1)}$ , we have

$$Z_{n+1} > \hat{Q}_n\{(1 + n^{-1})\alpha\} \text{ if and only if } Z_{n+1} > \hat{Q}_{n+1}(\alpha).$$

So,

$$\text{pr}[Z_{n+1} > \hat{Q}_n\{(1 + n^{-1})\alpha\}] = \text{pr}\{Z_{n+1} > \hat{Q}_{n+1}(\alpha)\} \geq 1 - \alpha,$$

and

$$\text{pr}[Z_{n+1} > \hat{Q}_n\{(1 + n^{-1})\alpha\}] = \text{pr}\{Z_{n+1} > \hat{Q}_{n+1}(\alpha)\} \leq 1 - \alpha + (n + 1)^{-1},$$

where the last inequality follows by applying Lemma 3 with  $n = n + 1$ .

□

## S5.1 Proof of Theorem 1

*Proof.* Let  $V_{n+1}$  be the score at the test point  $\mathbf{X}_{n+1}$  and  $k$  denote the smallest  $\lfloor (n_{cal}+1)(\alpha) \rfloor$  value in  $\{V_i; i \in \mathcal{I}_{cal}\}$ .

By construction of the prediction interval, we have that  $V_{n+1} > k$  is equivalent to

$$\begin{aligned} & \hat{f}(Y_{n+1} | \mathbf{X}_{n+1}) - c(\mathbf{X}_{n+1}) > k \\ \iff & \hat{f}(Y_{n+1} | \mathbf{X}_{n+1}) > k + c(\mathbf{X}_{n+1}) \\ \iff & Y_{n+1} \in \{y : \hat{f}(y | \mathbf{X}_{n+1}) > k + c(\mathbf{X}_{n+1})\}. \end{aligned}$$

So,

$$Y_{n+1} \in \hat{C}(\mathbf{X}_{n+1}) \iff V_{n+1} > k.$$

We then have that

$$pr\{Y_{n+1} \in \hat{C}(\mathbf{X}_{n+1})\} = pr(V_{n+1} > k).$$

Because the original pairs  $(\mathbf{X}_i, Y_i)$  are exchangeable, so are the scores  $V_i$  for  $i \in \mathcal{I}_{cal}$  and  $i = n + 1$ . So, by Lemma 4,

$$pr\{Y_{n+1} \in \hat{C}(\mathbf{X}_{n+1})\} \geq 1 - \alpha,$$

and, under the assumption that the  $V_i$ 's are almost surely distinct,

$$pr\{Y_{n+1} \in \hat{C}(\mathbf{X}_{n+1})\} \leq 1 - \alpha + (n_{cal} + 1)^{-1}.$$

□

## S5.2 Proof of Theorem 2

*Proof.* Recall  $0 < \alpha < 1$  is a fixed number. We first claim that:

**Claim 1:** it holds in probability that  $\hat{c}(\mathbf{x})$  converges to  $c(\mathbf{x})$ , uniformly in  $\mathbf{x}$  at the rate of  $b_{n_{train}}$ , as  $n_{train} \rightarrow \infty$ .

The proof of the claim will be given below. Assuming the validity of the preceding claim and

upon noting (C3), there exists a constant  $K$ , such that  $V_i = \hat{f}(Y_i | \mathbf{X}_i) - \hat{c}(\mathbf{X}_i) = \tilde{V}_i + \Delta_i$  where  $\tilde{V}_i = f(Y_i | \mathbf{X}_i) - c(\mathbf{X}_i)$  and  $|\Delta_i| \leq K \times b_{n_{train}}$ , with probability approaching 1, as  $n_{train} \rightarrow \infty$ . Consider the empirical distribution  $P_{V, n_{cal}} = \sum_{i=1}^{n_{cal}} n_{cal}^{-1} \delta_{V_i}$ , where  $\delta$  denotes the Dirac delta probability measure. Its Wasserstein distance from the empirical distribution  $P_{\tilde{V}, n_{cal}} = \sum_{i=1}^{n_{cal}} n_{cal}^{-1} \delta_{\tilde{V}_i}$  is less than  $K \times b_{n_{train}}$ , with probability approaching 1. Notice that  $P_{V, n_{cal}}$  converges weakly to the distribution of  $f(Y | \mathbf{X}) - c(\mathbf{X})$ . Note that the  $\alpha$  quantile  $P_{\tilde{V}, n_{cal}}$  converges to that of  $f(Y | \mathbf{X}) - c(\mathbf{X})$ , which is zero, at the rate of  $O_p(n_{cal}^{-1/2})$  [Van Der Vaart, 1998, Lemma 21.2], hence the stated order of the conformal adjustment  $\hat{q}$ .

It remains to verify Claim 1. First note that  $c(\mathbf{x})$  is a continuous function in  $\mathbf{x}$ . To see this, let  $\mathbf{x}_m \rightarrow \mathbf{x}$  as  $m \rightarrow \infty$  and let  $\tau_m$  be a sequence of positive numbers that approaches 0 as  $m \rightarrow \infty$ . Furthermore, write  $c_m$  for  $c(\mathbf{x}_m)$ . Let  $F(\cdot | \cdot)$  be the true conditional cdf, and  $\hat{F}(\cdot | \cdot)$  be that based on  $\hat{f}(\cdot | \cdot)$ . By the definition of  $c(\mathbf{x})$ , we have

$$\alpha - \tau_m < F(c_m | \mathbf{x}_m) \leq \alpha.$$

Thanks to assumptions 1 and 2,  $f(y | \mathbf{x})$  is a continuous and positive function. Consequently, for all  $\tau > 0$ ,  $F(c(\mathbf{x}) - \tau | \mathbf{x}) < \alpha < F(c(\mathbf{x}) + \tau | \mathbf{x})$ . It follows from assumptions 1 and 2 and a result of Scheffé [Van Der Vaart, 1998, Corollary 2.30] that  $F(c_m | \mathbf{x}_m) - F(c_m | \mathbf{x}) \rightarrow 0$ , as  $m \rightarrow \infty$ . We can then conclude that  $\limsup_m F(c_m | \mathbf{x}) \leq \limsup_m F(c_m | \mathbf{x}_m) + \lim_m \{F(c_m | \mathbf{x}) - F(c_m | \mathbf{x}_m)\} \leq \alpha$ , therefore  $c_m < c(\mathbf{x}) + \tau$  eventually. Similarly, we can show that  $\liminf F(c_m | \mathbf{x}) \geq \alpha$ , hence  $c_m > c(\mathbf{x} - \tau)$  eventually. Since  $\tau > 0$  is arbitrary, we conclude that  $c_m \rightarrow c(\mathbf{x})$  as  $m \rightarrow \infty$ . This completes the proof that  $c(\mathbf{x})$  is a continuous function of  $\mathbf{x}$ .

Next, we proceed to prove that  $\hat{c}(\mathbf{x})$  converges to  $c(\mathbf{x})$  uniformly in  $\mathbf{x} \in \mathcal{X}$ , at the rate of  $b_{n_{train}}$ , with probability approaching 1. Since  $\alpha$  is strictly between 0 and 1,  $c(\mathbf{x})$  lies in  $(a, b)$ , hence there exists  $\psi > 0$  such that  $\forall \mathbf{x} \in \mathcal{X}$ ,  $[c(\mathbf{x}) - \psi, c(\mathbf{x}) + \psi] \subset (a, b)$ . Since  $f(y | \mathbf{x})$  is a continuous, positive function, there exists a positive constant  $K_1$  such that  $f(\cdot | \mathbf{x})$  is bounded below by  $K_1$  over the interval  $[c(\mathbf{x}) - \psi, c(\mathbf{x}) + \psi]$ . Thus, for

all  $0 \leq \eta \leq \psi$ , we have  $F(c(\mathbf{x}) - \eta) \leq \alpha - K_1\eta$  and  $F(c(\mathbf{x}) + \eta) \geq \alpha + K_1\eta$ . Owing to assumption 3,  $\hat{F}(\cdot | \mathbf{x})$  converges to  $F(\cdot | \mathbf{x})$  in sup norm, at the rate of  $b_{n_{train}}$  uniformly in  $\mathbf{x} \in \mathcal{X}$ , with probability approaching 1. Thus, there exists another positive constant  $K_2$  such that for all  $0 \leq \eta \leq \psi$ , we have  $\hat{F}(c(\mathbf{x}) - \eta) \leq \alpha - K_1\eta + K_2b_{n_{train}}$  and  $\hat{F}(c(\mathbf{x}) + \eta) \geq \alpha + K_1\eta - K_2b_{n_{train}}$ , hence, for  $\eta = 2K_2K_1^{-1}b_{n_{train}}$ ,  $\hat{F}(c(\mathbf{x}) - \eta) < \alpha$  and  $\hat{F}(c(\mathbf{x}) + \eta) > \alpha$ , on an event with probability approaching 1. This shows that with probability approaching 1,  $|\hat{c}(\mathbf{x}) - c(\mathbf{x})| < 2K_2K_1^{-1}b_{n_{train}}$ . This completes the proof.  $\square$

### S5.3 Proof of Theorem 3

*Proof.* We first verify that  $c(\mathbf{x}; \theta)$  is a continuous function. Recall  $c(\mathbf{x}; \theta)$  is the unique solution to the equation  $H(\eta, \mathbf{x}, \theta) = 0$ . Now,  $\partial H / \partial \eta = f(\eta | \mathbf{x}; \theta) > 0$ , for any  $\eta$ . It follows from the implicit function theorem and assumption 6 that  $c(\mathbf{x}; \theta)$  is a continuously differentiable function of  $\mathbf{x}, \theta$ . Hence,  $c(\mathbf{x}; \hat{\theta}) \rightarrow c(\mathbf{x}; \theta_0)$  uniformly for  $\mathbf{x}$  in any fixed compact set, thanks to assumption 5.

Consider the empirical distribution  $P_{V, n_{cal}} = \sum_{i=1}^{n_{cal}} n_{cal}^{-1} \delta_{V_i}$ , where  $V_i = f(Y_i | \mathbf{X}_i; \hat{\theta}) - c(\mathbf{X}_i; \hat{\theta})$  and  $\delta$  denotes the Dirac delta probability measure. Next, we show that as  $n_{train} \rightarrow \infty$  and  $n_{cal} \rightarrow \infty$ ,  $P_{V, n_{cal}}$  converges weakly to the distribution of  $f(Y | \mathbf{X}; \theta_0) - c(\mathbf{X}; \theta_0)$ . It suffices to show that for any bounded continuous function  $g$ ,

$$\sum_{i=1}^{n_{cal}} g\{f(Y_i | \mathbf{X}_i; \hat{\theta}) - c(\mathbf{X}_i; \hat{\theta})\} / n \rightarrow E\{g(f(Y | \mathbf{X}; \theta_0) - c(\mathbf{X}; \theta_0))\}. \quad (\text{S5})$$

Let  $g$  be upper bounded by a constant  $M > 0$ . Let  $\epsilon > 0$  be given and  $\mathcal{R}$  be a compact set such that with probability greater than  $1 - \epsilon/M$ ,  $(Y, \mathbf{X}^\top)^\top \in \mathcal{R}$ . Decompose  $\sum_{i=1}^{n_{cal}} g\{f(Y_i | \mathbf{X}_i; \hat{\theta}) - c(\mathbf{X}_i; \hat{\theta})\} / n = S_1 + S_2 + S_3$  where

$$\begin{aligned} S_1 &= \sum_{i=1}^{n_{cal}} [g\{f(Y_i | \mathbf{X}_i; \hat{\theta}) - c(\mathbf{X}_i; \hat{\theta})\} - g\{f(Y_i | \mathbf{X}_i; \theta_0) - c(\mathbf{X}_i; \theta_0)\}] I\{(Y_i, \mathbf{X}_i^\top)^\top \in \mathcal{R}\} / n, \\ S_2 &= \sum_{i=1}^{n_{cal}} [g\{f(Y_i | \mathbf{X}_i; \hat{\theta}) - c(\mathbf{X}_i; \hat{\theta})\} - g\{f(Y_i | \mathbf{X}_i; \theta_0) - c(\mathbf{X}_i; \theta_0)\}] I\{(Y_i, \mathbf{X}_i^\top)^\top \notin \mathcal{R}\} / n, \\ S_3 &= \sum_{i=1}^{n_{cal}} g\{f(Y_i | \mathbf{X}_i; \theta_0) - c(\mathbf{X}_i; \theta_0)\} / n. \end{aligned}$$

Because of assumption 5,  $T_1 \rightarrow 0$ , almost surely, as  $n_{train} \rightarrow \infty$ . Note that  $T_2 \rightarrow E(T_2)$  and  $E(|T_2|) \leq \epsilon$ , while  $T_3 \rightarrow E\{g(f(Y | \mathbf{X}; \theta_0) - c(\mathbf{X}; \theta_0))\}$ , as  $n_{cal} \rightarrow \infty$ . Since  $\epsilon > 0$ , (S5) holds.

The preceding weak convergence result and assumption 4 then imply that the  $\alpha$  quantile of  $P_{\hat{V}, n_{cal}}$  converges to that of  $f(Y | \mathbf{X}; \theta_0) - c(\mathbf{X}; \theta_0)$ , which is zero [Van Der Vaart, 1998, Lemma 21.2], hence the conformal adjustment  $\hat{q} \rightarrow 0$ .  $\square$

## S6 Numerical Studies

As observed in Section 4 in the main text, all the other methods under cover in the tails. This is because, if we wanted to predict our response in the mixture scenario at  $X = 0.5$ , an observed data point with a covariate whose value is  $-0.5$  does not provide value because the conditional distributions are completely different. This is why the method that applied the heaviest local weight in the mixture scenario, KNN kernel conditional density estimator with our conformal adjustment, performed the best. KNN kernel conditional density estimation was also the only method to adapt to the smaller response values on the left end of the covariate distribution. This can be clearly seen on the left side of the plot in Figure S17.

In the asymmetric scenario, the conditional coverage seen in the left diagram in Figure 2 in the main text, where the coverage rates fall off in the tails of distributions, is common with conformal prediction [Lei and Wasserman, 2014, 2012]. It can be thought of as a bit of extrapolation, even though we observe data in the region. The smaller coverage can be seen well in Figure S8 and Figure S9. Even though we used a weighted regression technique to compute the FlexCode estimators, the density estimators that used larger local weights worked better. This can be seen in Figure S10 and Figure S11. Though, the techniques that use local weights do not always perform well in high dimensions [Wang and Scott, 2019]. Which is an important reminder to choose an appropriate conditional density estimator for

the given data.

Below, we include several displays of the simulation results.

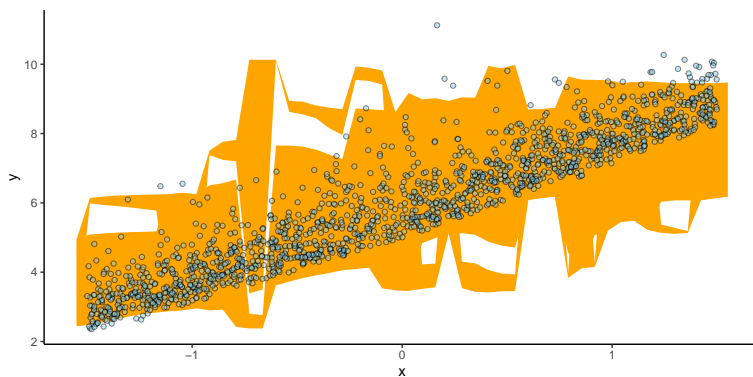


Figure S7: An example of the prediction regions given by Unadjusted (FlexCode) in the asymmetric scenario.

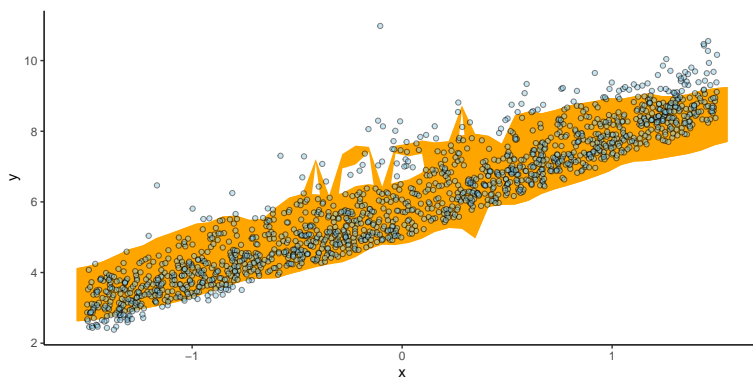


Figure S8: An example of the prediction regions given by HPD-split (FlexCode) in the asymmetric scenario.



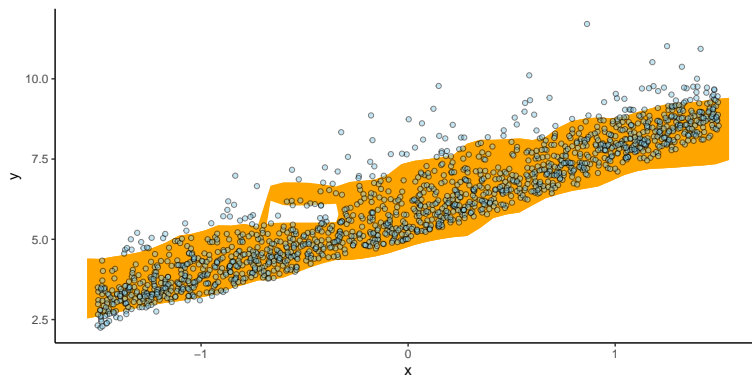


Figure S9: An example of the prediction regions given by CHCDS (FlexCode) in the asymmetric scenario.

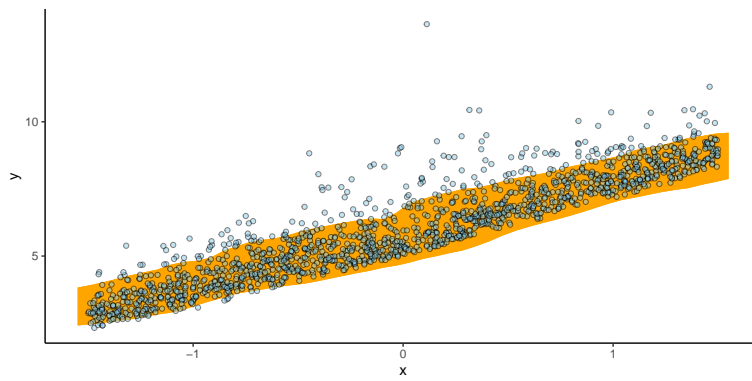


Figure S10: An example of the prediction regions given by CHCDS (Kernel) in the asymmetric scenario.

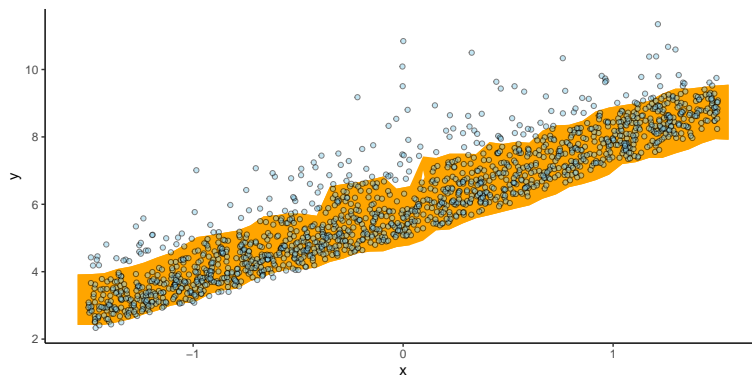


Figure S11: An example of the prediction regions given by CHCDS (KNN) in the asymmetric scenario.

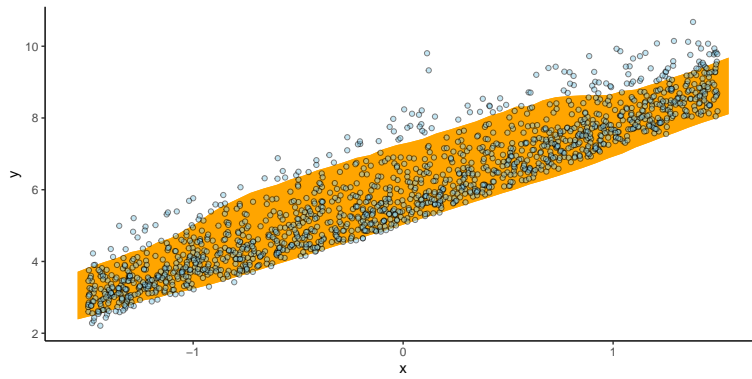


Figure S12: An example of the prediction regions given by CHCDS (Gaussian Mix) in the asymmetric scenario.

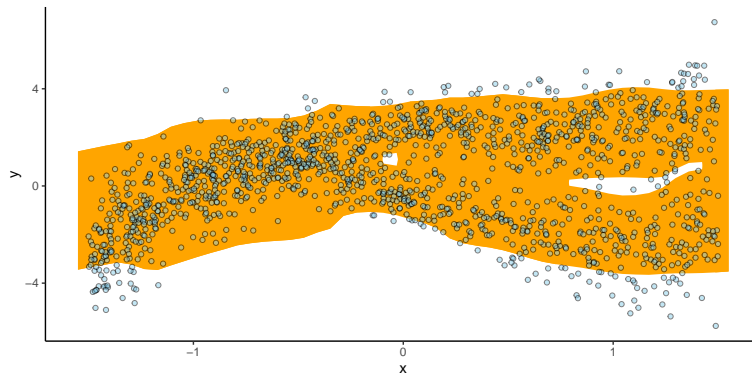


Figure S13: An example of the prediction regions given by Unadjusted (FlexCode) in the mixture scenario.

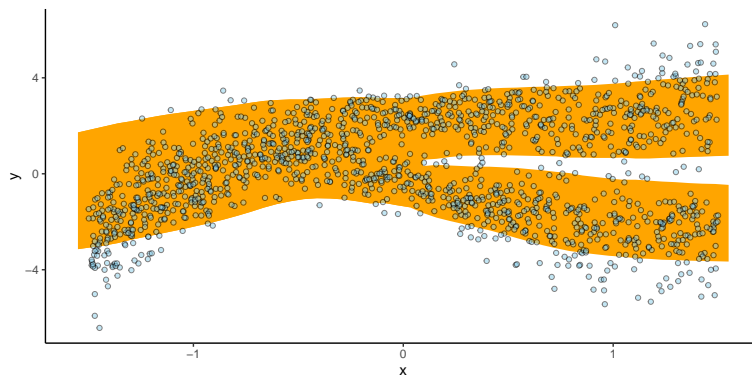


Figure S14: An example of the prediction regions given by HPD-split (FlexCode) in the mixture scenario.

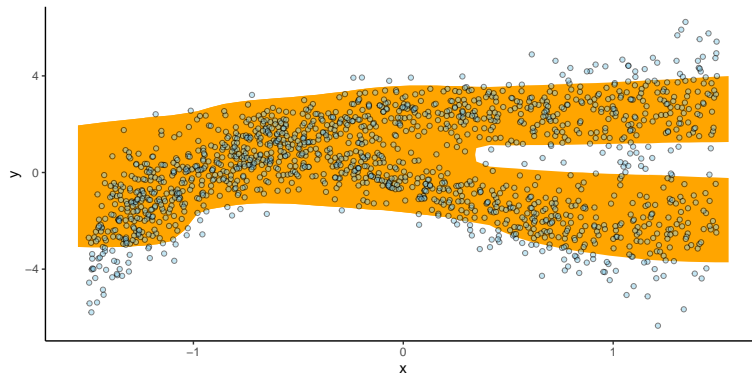


Figure S15: An example of the prediction regions given by CHCDS (FlexCode) in the mixture scenario.

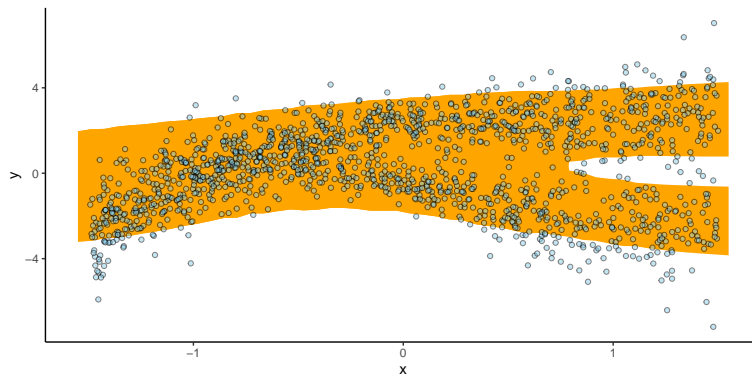


Figure S16: An example of the prediction regions given by CHCDS (Kernel) in the mixture scenario.

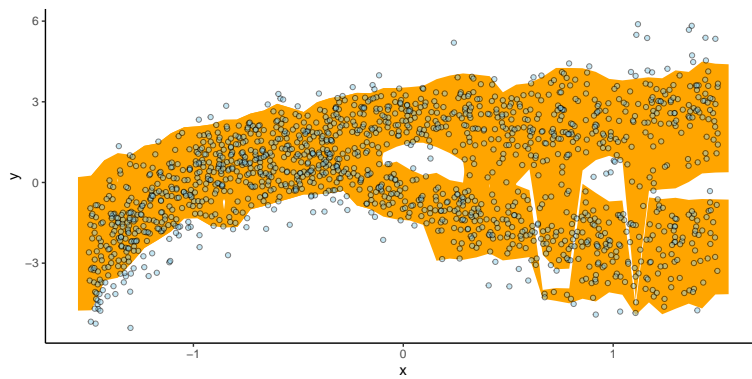


Figure S17: An example of the prediction regions given by CHCDS (KNN) in the mixture scenario.

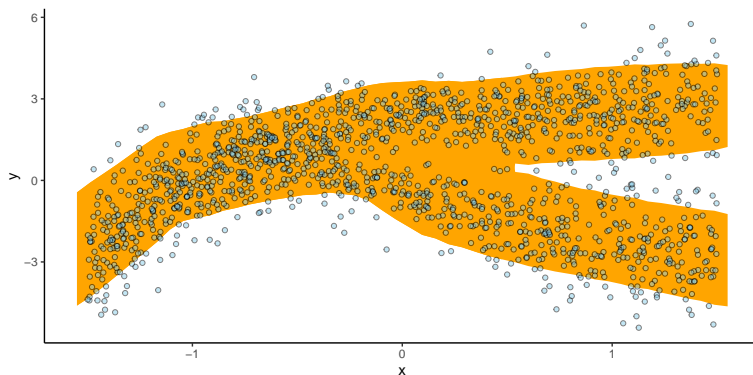


Figure S18: An example of the prediction regions given by CHCDS (Gaussian Mix) in the mixture scenario.

## S7 Further Real Analysis

To demonstrate the flexibility of CHCDS, we also created a conditional Gaussian mixture density estimator in Pytorch [Paszke et al., 2019]. We trained the model on 64,950 observations, computed calibration scores on 5,000 observations, and computed the coverage results on 5,000 out of sample observations. Those results can be found in Table 1. The feedforward model had 4 components, 3 hidden layers, and 2,652 parameters. The code can be found in a Jupyter notebook on GitHub [here](#).

Table 1: Coverage, conditional coverage, and average size of the prediction regions for CHCDS Pytorch conditional Gaussian mixture density estimator.

Coverage	Size
900 (4)	131 (13)
Coverage (Bright)	Size (Bright)
906 (6)	82
Coverage (Faint)	Size (Faint)
895 (6)	181 (3)

## References

- A. N. Angelopoulos and S. Bates. A gentle introduction to conformal prediction and distribution-free uncertainty quantification, 2021. URL <https://arxiv.org/abs/2107.07511>.
- R. Beck, C.-A. Lin, E. E. O. Ishida, F. Gieseke, R. S. de Souza, M. V. Costa-Duarte, M. W. Hattab, A. Krone-Martins, and for the COIN Collaboration. On the realistic validation of photometric redshifts. *Monthly Notices of the Royal Astronomical Society*, 468(4):4323–4339, 03 2017. ISSN 0035-8711. doi: 10.1093/mnras/stx687. URL <https://doi.org/10.1093/mnras/stx687>.
- C. Bishop. Mixture density networks. Workingpaper, Aston University, 1994.
- T. Cacoullos. Estimation of a multivariate density. *Annals of the Institute of Statistical Mathematics*, 18:179–189, 1966. doi: <https://doi.org/10.1007/BF02869528>. URL <https://www.sciencedirect.com/science/article/pii/0047259X79900654>.
- M. Carrasco Kind and R. J. Brunner. TPZ: photometric redshift PDFs and ancillary information by using prediction trees and random forests. *Monthly Notices of the Royal Astronomical Society*, 432(2):1483–1501, 05 2013. ISSN 0035-8711. doi: 10.1093/mnras/stt574. URL <https://doi.org/10.1093/mnras/stt574>.
- B. Chassagnol, A. Bichat, C. Boudjeniba, P.-H. Wuillemin, M. Guedj, D. Gohel, G. Nuel, and E. Becht. Gaussian mixture models in r. *The R Journal*, 15:56–76, 2023. ISSN 2073-4859. doi: 10.32614/RJ-2023-043. <https://doi.org/10.32614/RJ-2023-043>.
- Y.-C. Chen, C. R. Genovese, and L. Wasserman. Density level sets: Asymptotics, inference, and visualization. *Journal of the American Statistical Association*, 112(520): 1684–1696, 2017. doi: 10.1080/01621459.2016.1228536. URL <https://doi.org/10.1080/01621459.2016.1228536>.

- S.-T. Chiu. A comparative review of bandwidth selection for kernel density estimation. *Statistica Sinica*, 6(1):129–145, 1996. ISSN 10170405, 19968507. URL <http://www.jstor.org/stable/24306003>.
- A. Cuevas and R. Fraiman. A plug-in approach to support estimation. *The Annals of Statistics*, 25(6):2300–2312, 1997. ISSN 00905364. URL <http://www.jstor.org/stable/2959033>.
- N.-B. Heidenreich, A. Schindler, and S. Sperlich. Bandwidth selection for kernel density estimation: a review of fully automatic selectors. *AStA Advances in Statistical Analysis*, 97(4):403–433, 2013. URL <https://EconPapers.repec.org/RePEc:spr:alstar:v:97:y:2013:i:4:p:403-433>.
- K. Hirano and G. W. Imbens. *The Propensity Score with Continuous Treatments*, chapter 7, pages 73–84. John Wiley & Sons, Ltd, 2004. ISBN 9780470090459. doi: <https://doi.org/10.1002/0470090456.ch7>. URL <https://onlinelibrary.wiley.com/doi/abs/10.1002/0470090456.ch7>.
- R. J. Hyndman, D. M. Bashtannyk, and G. K. Grunwald. Estimating and visualizing conditional densities. *Journal of Computational and Graphical Statistics*, 5(4):315–336, 1996. ISSN 10618600. URL <http://www.jstor.org/stable/1390887>.
- R. Izbicki and A. B. Lee. Nonparametric conditional density estimation in a high-dimensional regression setting. *Journal of Computational and Graphical Statistics*, 25(4):1297–1316, 2016. ISSN 10618600, 15372715. URL <http://www.jstor.org/stable/44861921>.
- R. Izbicki and A. B. Lee. Converting high-dimensional regression to high-dimensional conditional density estimation. *Electronic Journal of Statistics*, 11:2800 – 2831, 04 2017. doi: 10.1214/17-EJS1302.

- R. Izbicki, A. B. Lee, and T. Pospisil. Abc–cde: Toward approximate bayesian computation with complex high-dimensional data and limited simulations. *Journal of Computational and Graphical Statistics*, 28(3):481–492, 2019. doi: 10.1080/10618600.2018.1546594. URL <https://doi.org/10.1080/10618600.2018.1546594>.
- R. Izbicki, G. Shimizu, and R. Stern. Flexible distribution-free conditional predictive bands using density estimators. In *Proceedings of the Twenty Third International Conference on Artificial Intelligence and Statistics*, volume 108 of *Proceedings of Machine Learning Research*, pages 3068–3077. PMLR, 08 2020. URL <https://proceedings.mlr.press/v108/izbicki20a.html>.
- R. Izbicki, G. Shimizu, and R. B. Stern. Cd-split and hpd-split: Efficient conformal regions in high dimensions. *Journal of Machine Learning Research*, 23(87):1–32, 2022. URL <http://jmlr.org/papers/v23/20-797.html>.
- H. Jiang. Uniform convergence rates for kernel density estimation. In D. Precup and Y. W. Teh, editors, *Proceedings of the 34th International Conference on Machine Learning*, volume 70 of *Proceedings of Machine Learning Research*, pages 1694–1703. PMLR, 08 2017. URL <https://proceedings.mlr.press/v70/jiang17b.html>.
- D. P. Kingma, T. Salimans, R. Jozefowicz, X. Chen, I. Sutskever, and M. Welling. Improved variational inference with inverse autoregressive flow. In *Advances in Neural Information Processing Systems*, volume 29. Curran Associates, Inc., 2016. URL [https://proceedings.neurips.cc/paper\\_files/paper/2016/file/ddeebdeefdb7e7e7a697e1c3e3d8ef54-Paper.pdf](https://proceedings.neurips.cc/paper_files/paper/2016/file/ddeebdeefdb7e7e7a697e1c3e3d8ef54-Paper.pdf).
- I. Kobyzev, S. D. Prince, and M. A. Brubaker. Normalizing flows: An introduction and review of current methods. *IEEE Transactions on Pattern Analysis & Machine Intelligence*, 43(11):3964–3979, 11 2021. ISSN 1939-3539. doi: 10.1109/TPAMI.2020.2992934.

- R. Kumar, C. Carroll, A. Hartikainen, and O. Martin. Arviz a unified library for exploratory analysis of bayesian models in python. *Journal of Open Source Software*, 4(33):1143, 2019. doi: 10.21105/joss.01143. URL <https://doi.org/10.21105/joss.01143>.
- J. Lei and L. Wasserman. Distribution free prediction bands, 2012. URL <https://arxiv.org/abs/1203.5422>.
- J. Lei and L. Wasserman. Distribution-free prediction bands for non-parametric regression. *Journal of the Royal Statistical Society Series B*, 76(1):71–96, 1 2014. URL <https://ideas.repec.org/a/bla/jorssb/v76y2014i1p71-96.html>.
- J. Lei, M. G’Sell, A. Rinaldo, R. J. Tibshirani, and L. Wasserman. Distribution-free predictive inference for regression. *Journal of the American Statistical Association*, 113 (523):1094–1111, 2018. doi: 10.1080/01621459.2017.1307116. URL <https://doi.org/10.1080/01621459.2017.1307116>.
- D. O. Loftsgaarden and C. P. Quesenberry. A Nonparametric Estimate of a Multivariate Density Function. *The Annals of Mathematical Statistics*, 36(3):1049 – 1051, 1965. doi: 10.1214/aoms/1177700079. URL <https://doi.org/10.1214/aoms/1177700079>.
- Y. Mack and M. Rosenblatt. Multivariate k-nearest neighbor density estimates. *Journal of Multivariate Analysis*, 9(1):1–15, 1979. ISSN 0047-259X. doi: [https://doi.org/10.1016/0047-259X\(79\)90065-4](https://doi.org/10.1016/0047-259X(79)90065-4). URL <https://www.sciencedirect.com/science/article/pii/0047259X79900654>.
- D. S. Moore and J. W. Yackel. Consistency Properties of Nearest Neighbor Density Function Estimators. *The Annals of Statistics*, 5(1):143 – 154, 1977. doi: 10.1214/aos/1176343747. URL <https://doi.org/10.1214/aos/1176343747>.
- G. Papamakarios, T. Pavlakou, and I. Murray. Masked autoregressive flow for density estimation. In I. Guyon, U. V. Luxburg, S. Bengio, H. Wallach, R. Fergus, S. Vishwanathan,



- and R. Garnett, editors, *Advances in Neural Information Processing Systems*, volume 30. Curran Associates, Inc., 2017. URL [https://proceedings.neurips.cc/paper\\_files/paper/2017/file/6c1da886822c67822bcf3679d04369fa-Paper.pdf](https://proceedings.neurips.cc/paper_files/paper/2017/file/6c1da886822c67822bcf3679d04369fa-Paper.pdf).
- G. Papamakarios, E. Nalisnick, D. J. Rezende, S. Mohamed, and B. Lakshminarayanan. Normalizing flows for probabilistic modeling and inference. *Journal of Machine Learning Research*, 22(57):1–64, 2021. URL <http://jmlr.org/papers/v22/19-1028.html>.
- E. Parzen. On Estimation of a Probability Density Function and Mode. *The Annals of Mathematical Statistics*, 33(3):1065 – 1076, 1962. doi: 10.1214/aoms/1177704472. URL <https://doi.org/10.1214/aoms/1177704472>.
- A. Paszke, S. Gross, F. Massa, A. Lerer, J. Bradbury, G. Chanan, T. Killeen, Z. Lin, N. Gimelshein, L. Antiga, A. Desmaison, A. Köpf, E. Yang, Z. DeVito, M. Raison, A. Tejani, S. Chilamkurthy, B. Steiner, L. Fang, J. Bai, and S. Chintala. Pytorch: An imperative style, high-performance deep learning library, 2019.
- W. Polonik. Measuring Mass Concentrations and Estimating Density Contour Clusters-An Excess Mass Approach. *The Annals of Statistics*, 23(3):855 – 881, 1995. doi: 10.1214/aos/1176324626. URL <https://doi.org/10.1214/aos/1176324626>.
- R Core Team. *R: A Language and Environment for Statistical Computing*. R Foundation for Statistical Computing, Vienna, Austria, 2023. URL <https://www.R-project.org/>.
- D. Rezende and S. Mohamed. Variational inference with normalizing flows. In F. Bach and D. Blei, editors, *Proceedings of the 32nd International Conference on Machine Learning*, volume 37 of *Proceedings of Machine Learning Research*, pages 1530–1538, Lille, France, 7 2015. PMLR. URL <https://proceedings.mlr.press/v37/rezende15.html>.
- P. Rigollet and R. Vert. Optimal rates for plug-in estimators of density level sets. *Bernoulli*,

- 15(4), Nov. 2009. ISSN 1350-7265. doi: 10.3150/09-bej184. URL <http://dx.doi.org/10.3150/09-BEJ184>.
- Y. Romano, E. Patterson, and E. Candes. Conformalized quantile regression. In *Advances in Neural Information Processing Systems*, volume 32. Curran Associates, Inc., 2019. URL [https://proceedings.neurips.cc/paper\\_files/paper/2019/file/5103c3584b063c431bd1268e9b5e76fb-Paper.pdf](https://proceedings.neurips.cc/paper_files/paper/2019/file/5103c3584b063c431bd1268e9b5e76fb-Paper.pdf).
- M. Rosenblatt. Remarks on Some Nonparametric Estimates of a Density Function. *The Annals of Mathematical Statistics*, 27(3):832–837, 1956. doi: 10.1214/aoms/1177728190. URL <https://doi.org/10.1214/aoms/1177728190>.
- M. Rosenblatt. Curve estimates. *The Annals of Mathematical Statistics*, 42(6):1815–1842, 1971. ISSN 00034851. URL <http://www.jstor.org/stable/2240110>.
- J. Rothfuss, F. Ferreira, S. Boehm, S. Walther, M. Ulrich, T. Asfour, and A. Krause. Noise regularization for conditional density estimation. *arXiv:1907.08982*, 2019.
- R. J. Samworth and M. P. Wand. Asymptotics and optimal bandwidth selection for highest density region estimation. *The Annals of Statistics*, 38(3), 06 2010. ISSN 0090-5364. doi: 10.1214/09-aos766. URL <http://dx.doi.org/10.1214/09-AOS766>.
- L. Scrucca, C. Fraley, T. B. Murphy, and A. E. Raftery. *Model-Based Clustering, Classification, and Density Estimation Using mclust in R*. Chapman and Hall/CRC, 2023. ISBN 978-1032234953. doi: 10.1201/9781003277965. URL <https://mclust-org.github.io/book/>.
- E. S. Sheldon, C. E. Cunha, R. Mandelbaum, J. Brinkmann, and B. A. Weaver. Photometric redshift probability distributions for galaxies in the sdss dr8. *The Astrophysical Journal Supplement Series*, 201(2):32, aug 2012. doi: 10.1088/0067-0049/201/2/32. URL <http://dx.doi.org/10.1088/0067-0049/201/2/32>.

- R. J. Tibshirani, R. Foygel Barber, E. Candes, and A. Ramdas. Conformal prediction under covariate shift. In *Advances in Neural Information Processing Systems*, volume 32. Curran Associates, Inc., 2019. URL [https://proceedings.neurips.cc/paper\\_files/paper/2019/file/8fb21ee7a2207526da55a679f0332de2-Paper.pdf](https://proceedings.neurips.cc/paper_files/paper/2019/file/8fb21ee7a2207526da55a679f0332de2-Paper.pdf).
- B. L. Trippe and R. E. Turner. Conditional density estimation with bayesian normalising flows, 2018.
- A. Van Der Vaart. *Asymptotic Statistics*. Cambridge Series in Statistical and Probabilistic Mathematics, 3. Cambridge University Press, 1998. ISBN 9780521496032. URL <https://books.google.com/books?id=udhfQgAACAAJ>.
- C. Viroli and G. J. McLachlan. Deep gaussian mixture models. *Statistics and Computing*, 29(1):43–51, Jan. 2019.
- V. Vovk. Conditional validity of inductive conformal predictors. In *Proceedings of the Asian Conference on Machine Learning*, volume 25 of *Proceedings of Machine Learning Research*, pages 475–490, Singapore Management University, Singapore, 11 2012. PMLR. URL <https://proceedings.mlr.press/v25/vovk12.html>.
- V. Vovk, A. Gammerman, and G. Shafer. *Algorithmic Learning in a Random World*. Springer-Verlag, Berlin, Heidelberg, 2005. ISBN 0387001522.
- Z. Wang and D. W. Scott. Nonparametric density estimation for high-dimensional data—algorithms and applications. *WIREs Computational Statistics*, 11(4):e1461, 2019. doi: <https://doi.org/10.1002/wics.1461>. URL <https://wires.onlinelibrary.wiley.com/doi/abs/10.1002/wics.1461>.
- C. Winkler, D. Worrall, E. Hoogeboom, and M. Welling. Learning likelihoods with conditional normalizing flows, 2023.